

Unbiased Hamiltonian Monte Carlo with couplings

Jeremy Heng* and Pierre E. Jacob*

December 14, 2024

Abstract

We propose a methodology to parallelize Hamiltonian Monte Carlo estimators. Our approach constructs a pair of Hamiltonian Monte Carlo chains that are coupled in such a way that they meet exactly after some random number of iterations. These chains can then be combined so that resulting estimators are unbiased. This allows us to produce independent replicates in parallel and average them to obtain estimators that are consistent in the limit of the number of replicates, instead of the usual limit of the number of Markov chain iterations. The choice of algorithmic parameters and the efficiency of our proposed methodology are illustrated on a truncated Gaussian distribution, a logistic regression with 300 covariates, and a log-Gaussian Cox point processes model with a finely grained discretization.

Keywords: Coupling, Hamiltonian Monte Carlo, Parallel computing, Unbiased estimation.

1 Introduction

1.1 Parallel computation with Hamiltonian Monte Carlo

Hamiltonian Monte Carlo is a Markov chain Monte Carlo method to approximate integrals with respect to a target probability distribution π on \mathbb{R}^d . Originally proposed by [Duane et al. \[1987\]](#) in the physics literature, it was later introduced in statistics by [Neal \[1993\]](#) and is now widely adopted as a standard sampling tool [[Brooks et al., 2011](#), [Lelièvre et al., 2010](#)]. Moreover, its theoretical properties are now better understood: see [Beskos et al. \[2013\]](#) and [Mangoubi and Smith \[2017\]](#) for scaling results with respect to dimension, [Betancourt et al. \[2017\]](#) and [Betancourt \[2017\]](#) for its geometric properties. In practice, Hamiltonian Monte Carlo is at the core of the No-U-Turn sampler [[Hoffman and Gelman, 2014](#)] implemented in the software Stan [[Carpenter et al., 2016](#)].

If one could initialize from the target distribution, usual estimators based on any Markov chain Monte Carlo would be unbiased, and one could simply average over independent chains [[Rosenthal, 2000](#)]. Except certain applications where this can be achieved with perfect simulation methods [[Casella et al., 2001](#), [Huber, 2016](#)], estimators based on Markov chain Monte Carlo are ultimately justified in the limit of the number of iterations. Algorithms that rely on such asymptotics face the risk of becoming obsolete if computational power continue to increase through the number of available processors and not through clock speed.

Several methods have been proposed to address this limitation with varying generality [[Mykland et al., 1995](#), [Neal, 2002](#), [Glynn and Rhee, 2014](#)]. Our approach builds upon recent work by [Jacob et al. \[2017\]](#), which introduces unbiased estimators based on Metropolis–Hastings algorithms and Gibbs samplers. The present article describes how to design unbiased estimators for Hamiltonian Monte Carlo and some of its variants [[Girolami and Calderhead, 2011](#)]. The proposed methodology is widely applicable and involves a

*Department of Statistics, Harvard University, USA. Emails: jjmheng@fas.harvard.edu & pjacob@fas.harvard.edu.

simple coupling between a pair of Hamiltonian Monte Carlo chains. Coupled chains are run for a random but almost surely finite number of iterations, and combined in such a way that resulting estimators are unbiased. One can produce independent copies of these estimators in parallel and average them to obtain consistent approximations in the limit of the number of replicates. This also yields confidence intervals valid in the number of replicates through the central limit theorem.

We begin by introducing some preliminary notation in Section 1.2 and recapitulating the unbiased estimation framework of [Jacob et al. \[2017\]](#) in Section 1.3. An R package implementing the numerical results of this article is available on the GitHub account of the second author¹. The proofs of all results are given in Appendix B–C.

1.2 Notation

Given a sequence $(x_n)_{n \geq 0}$ and integers $k < m$, we use the convention that $\sum_{n=m}^k x_n = 0$. The set of natural numbers is denoted by \mathbb{N} and the set of non-negative real numbers by \mathbb{R}_+ . The d -dimensional vector of zeros is denoted by 0_d and the $d \times d$ identity matrix by I_d . The Euclidean norm of a vector $x \in \mathbb{R}^d$ is written as $|x| = (\sum_{i=1}^d x_i^2)^{1/2}$. Given a subset $A \subseteq \Omega$, the indicator function $\mathbb{I}_A : \Omega \rightarrow \{0, 1\}$ is defined as $\mathbb{I}_A(x) = 1$ if $x \in A$, and 0 if $x \in \Omega \setminus A$. For a smooth function $f : \mathbb{R}^d \rightarrow \mathbb{R}$, we denote its gradient by $\nabla f : \mathbb{R}^d \rightarrow \mathbb{R}^d$ and its Hessian by $\nabla^2 f : \mathbb{R}^d \rightarrow \mathbb{R}^{d \times d}$. The gradient of a function $(x, y) \mapsto f(x, y)$ with respect to the variables x and y are denoted by $\nabla_x f$ and $\nabla_y f$ respectively. The Borel σ -algebra of \mathbb{R}^d is denoted by $\mathcal{B}(\mathbb{R}^d)$; on the product space $\mathbb{R}^d \times \mathbb{R}^d$, $\mathcal{B}(\mathbb{R}^d) \times \mathcal{B}(\mathbb{R}^d)$ denotes the product σ -algebra. The Gaussian distribution on \mathbb{R}^d with mean vector μ and covariance matrix Σ is denoted by $\mathcal{N}(\mu, \Sigma)$, and its density by $x \mapsto \mathcal{N}(x; \mu, \Sigma)$. The uniform distribution on $[0, 1]$ is denoted as $\mathcal{U}[0, 1]$. We use the shorthand $X \sim \eta$ to refer to a random variable with distribution η . On a measurable space (Ω, \mathcal{F}) , given a measurable function $\varphi : \Omega \rightarrow \mathbb{R}$, a probability measure η , and a Markov transition kernel M , we define the integral $\eta(\varphi) = \int_{\Omega} \varphi(x) \eta(dx)$ and the function $M(\varphi)(x) = \int_{\Omega} \varphi(y) M(x, dy)$ for $x \in \Omega$.

1.3 Unbiased estimation with couplings

Suppose $h : \mathbb{R}^d \rightarrow \mathbb{R}$ is a measurable function of interest and consider the task of approximating the integral $\pi(h) = \int h(x) \pi(dx) < \infty$. Following [Glynn and Rhee \[2014\]](#) and [Jacob et al. \[2017\]](#), we will construct a pair of coupled Markov chains $X = (X_n)_{n \geq 0}$ and $Y = (Y_n)_{n \geq 0}$ with the same marginal law, associated with an initial distribution π_0 and a π -invariant Markov transition kernel K defined on $(\mathbb{R}^d, \mathcal{B}(\mathbb{R}^d))$. To do so, we introduce a Markov transition kernel \bar{K} on $(\mathbb{R}^d \times \mathbb{R}^d, \mathcal{B}(\mathbb{R}^d) \times \mathcal{B}(\mathbb{R}^d))$ that admits K as its marginals, i.e. $\bar{K}((x, y), A \times \mathbb{R}^d) = K(x, A)$ and $\bar{K}((x, y), \mathbb{R}^d \times A) = K(y, A)$ for all $x, y \in \mathbb{R}^d$ and $A \in \mathcal{B}(\mathbb{R}^d)$. After initializing $(X_0, Y_0) \sim \bar{\pi}_0$ with a coupling that has π_0 as its marginals, we then simulate $X_1 \sim K(X_0, \cdot)$ and $(X_{n+1}, Y_n) \sim \bar{K}((X_n, Y_{n-1}), \cdot)$ for all integer $n \geq 1$. We will write \mathbb{P} to denote the law of the coupled chain $(X_n, Y_n)_{n \geq 0}$, and \mathbb{E} to denote expectation with respect to \mathbb{P} . We now consider the following assumptions.

Assumption 1 (Convergence of marginal chain). *As $n \rightarrow \infty$, we have $\mathbb{E}[h(X_n)] \rightarrow \pi(h)$. Furthermore, there exist $\kappa_1 > 0$ and $C_1 < \infty$ such that $\mathbb{E}[h(X_n)^{2+\kappa_1}] < C_1$ for all integer $n \geq 0$.*

Assumption 2 (Tail of meeting time). *The meeting time $\tau = \inf\{n \geq 1 : X_n = Y_{n-1}\}$ satisfies a geometric tail condition of the form $\mathbb{P}(\tau > n) \leq C_2 \kappa_2^n$ for some constants $C_2 \in \mathbb{R}_+$, $\kappa_2 \in (0, 1)$ and all integer $n \geq 0$.*

Assumption 3 (Faithfulness). *The coupled chains are faithful [Rosenthal, 1997], i.e. $X_n = Y_{n-1}$ for all integer $n \geq \tau$.*

¹Link: github.com/pierrejacob/debiasedhmc.

Under these assumptions, the random variable defined as

$$H_k(X, Y) = h(X_k) + \sum_{n=k+1}^{\tau-1} \{h(X_n) - h(Y_{n-1})\} \quad (1)$$

for any integer $k \geq 0$, is an unbiased estimator of $\pi(h)$ with finite variance [Jacob et al., 2017, Proposition 3.1]. Computation of (1) can be performed with τ applications of \bar{K} and $\max(1, k+1-\tau)$ applications of K ; thus the compute cost has a finite expectation under Assumption 2. The first term, $h(X_k)$, is in general biased since the chain $(X_n)_{n \geq 0}$ might not have reached stationarity by iteration k . The second term acts as a bias correction and is equal to zero when $k \geq \tau-1$.

As the estimators $H_k(X, Y)$, for various values of k , can be computed from a single realization of the coupled chain, this prompts the definition of a time-averaged estimator $H_{k:m}(X, Y) = (m-k+1)^{-1} \sum_{n=k}^m H_n(X, Y)$ for integers $k \leq m$. The latter inherits the unbiasedness and finite variance properties, and can be rewritten as

$$H_{k:m}(X, Y) = M_{k:m}(X) + \sum_{n=k+1}^{\tau-1} \min\left(1, \frac{n-k}{m-k+1}\right) \{h(X_n) - h(Y_{n-1})\} \quad (2)$$

where $M_{k:m}(X) = (m-k+1)^{-1} \sum_{n=k}^m h(X_n)$ can be viewed as the usual Markov chain estimator with m iterations and a burn-in period of $k-1$. As before, the second term plays the role of bias correction and is equal to zero when $k \geq \tau-1$. Hence if the value of k is sufficiently large, we can expect the variance of $H_{k:m}(X, Y)$ to be close to that of $M_{k:m}(X)$. Moreover, the cost of computing (2), which involves τ applications of \bar{K} and $\max(1, m+1-\tau)$ applications of K , becomes comparable to m iterations under K for sufficiently large m . Therefore we can expect the asymptotic inefficiency of $H_{k:m}(X, Y)$ in the limit of our computational budget, given by the product of the expected compute cost and the variance of $H_{k:m}(X, Y)$ [Glynn and Whitt, 1992], to approach the asymptotic variance of the underlying Markov chain as m increases. We refer to Jacob et al. [2017, Section 3.1] for a more detailed discussion on the impact of k and m , and recall their proposed guideline of having k as a large quantile of the meeting time τ and m as a large multiple of k . Most importantly, unbiasedness of (2) allows one to easily exploit parallel computing architectures by producing R independent replicates $H_{k:m}^{(r)}(X, Y)$, $r = 1, \dots, R$ in parallel, and compute the average $R^{-1} \sum_{r=1}^R H_{k:m}^{(r)}(X, Y)$ to approximate $\pi(h)$. By appealing to the usual central limit theorem for independent and identically distributed random variables, confidence intervals that are justified as $R \rightarrow \infty$ can also be constructed.

Explicit construction of coupled chains satisfying Assumptions 1–3 for Markov kernels K that are defined by Metropolis–Hastings algorithms and Gibbs samplers are given in Jacob et al. [2017, Section 4]. The focus of this article is to propose a coupling strategy that is tailored for Hamiltonian Monte Carlo chains, so as to enable the use of unbiased estimators (1)–(2).

2 Hamiltonian dynamics

2.1 Hamiltonian flows

Suppose that the target distribution has the form $\pi(dq) \propto \exp\{-U(q)\}dq$, where the potential function $U : \mathbb{R}^d \rightarrow \mathbb{R}_+$ satisfies the following assumptions.

Assumption 4 (Regularity of potential). *The potential U is twice continuously differentiable and its gradient $\nabla U : \mathbb{R}^d \rightarrow \mathbb{R}^d$ is globally β -Lipschitz, i.e. there exists $\beta > 0$ such that*

$$|\nabla U(q) - \nabla U(q')| \leq \beta|q - q'|$$

for all $q, q' \in \mathbb{R}^d$.

We now introduce Hamiltonian flows on the phase space $\mathbb{R}^d \times \mathbb{R}^d$, which consists of position variables $q \in \mathbb{R}^d$ and momentum variables $p \in \mathbb{R}^d$. We will be concerned with a Hamiltonian function $E : \mathbb{R}^d \times \mathbb{R}^d \rightarrow \mathbb{R}_+$ of the form $E(q, p) = U(q) + |p|^2/2$. We note the use of the identity mass matrix here and will rely on preconditioning in Section 5.4 to incorporate curvature properties of π . The time evolution of a particle $(q(t), p(t))_{t \in \mathbb{R}_+}$ under Hamiltonian dynamics is described by the ordinary differential equations

$$\frac{d}{dt}q(t) = \nabla_p E(q(t), p(t)) = p(t), \quad \frac{d}{dt}p(t) = -\nabla_q E(q(t), p(t)) = -\nabla U(q(t)). \quad (3)$$

Under Assumption 4, (3) with an initial condition $(q(0), p(0)) = (q_0, p_0) \in \mathbb{R}^d \times \mathbb{R}^d$ admits a unique solution globally on \mathbb{R}_+ [Lelièvre et al., 2010, p. 14]. Therefore the flow map $\Phi_t(q_0, p_0) = (q(t), p(t))$ is well-defined for any $t \in \mathbb{R}_+$, and we will write its projection onto the position and momentum coordinates as $\Phi_t^\circ(q_0, p_0) = q(t)$ and $\Phi_t^*(q_0, p_0) = p(t)$ respectively.

It is worth recalling that Hamiltonian flows have the following properties.

Property 1 (Reversibility). *For any $t \in \mathbb{R}_+$, the inverse flow map satisfies $\Phi_t^{-1} = M \circ \Phi_t \circ M$, where $M(q, p) = (q, -p)$ denotes momentum reversal.*

Property 2 (Energy conservation). *The Hamiltonian function satisfies $E \circ \Phi_t = E$ for any $t \in \mathbb{R}_+$.*

Property 3 (Volume preservation). *For any $t \in \mathbb{R}_+$ and $A \in \mathcal{B}(\mathbb{R}^{2d})$, we have $\text{Leb}_{2d}\{\Phi_t(A)\} = \text{Leb}_{2d}(A)$, where Leb_{2d} denotes the Lebesgue measure on \mathbb{R}^{2d} .*

These properties imply that the extended target distribution on phase space $\tilde{\pi}(dq, dp) \propto \exp\{-E(q, p)\}dqdp$ is invariant under the Markov semi-group induced by the flow, i.e. for any $t \in \mathbb{R}_+$, the pushforward measure $\Phi_t\#\tilde{\pi}$, defined as $\Phi_t\#\tilde{\pi}(A) = \tilde{\pi}\{\Phi_t^{-1}(A)\}$ for $A \in \mathcal{B}(\mathbb{R}^{2d})$, is equal to $\tilde{\pi}$.

2.2 Coupled Hamiltonian dynamics

We now consider the coupling of two particles $(q^i(t), p^i(t))_{t \in \mathbb{R}_+}$, ($i = 1, 2$) evolving under (3) with initial conditions $(q^i(0), p^i(0)) = (q_0^i, p_0^i)$, ($i = 1, 2$). We first draw some insights from a Gaussian example.

Example 1. Let π be a Gaussian distribution on \mathbb{R} with mean $\mu \in \mathbb{R}$ and variance $\sigma^2 > 0$. In this case, we have $U(q) = (q - \mu)^2/(2\sigma^2)$, $\nabla U(q) = (q - \mu)/\sigma^2$ and the solution of (3) is

$$\Phi_t(q_0, p_0) = \begin{pmatrix} \mu + (q_0 - \mu) \cos\left(\frac{t}{\sigma}\right) + \sigma p_0 \sin\left(\frac{t}{\sigma}\right) \\ p_0 \cos\left(\frac{t}{\sigma}\right) - \frac{1}{\sigma}(q_0 - \mu) \sin\left(\frac{t}{\sigma}\right) \end{pmatrix}.$$

Hence the difference between particle positions is

$$q^1(t) - q^2(t) = (q_0^1 - q_0^2) \cos\left(\frac{t}{\sigma}\right) + \sigma(p_0^1 - p_0^2) \sin\left(\frac{t}{\sigma}\right).$$

If we set $p_0^1 = p_0^2$, then $|q^1(t) - q^2(t)| = \cos(t/\sigma)|q_0^1 - q_0^2|$, so for any non-negative integer n , the particles meet exactly whenever $t = (2n + 1)\pi\sigma/2$, and contraction occurs for any $t \neq \pi n\sigma$.

This example motivates a coupling that simply assigns particles the same initial momentum. Moreover, it also reveals that certain trajectory lengths will result in larger contraction than others. We now examine the utility of this approach more generally. Define $\Delta(t) = q^1(t) - q^2(t)$ as the difference between particle locations and note that

$$\frac{1}{2} \frac{d}{dt} |\Delta(t)|^2 = \Delta(t)^\top \{p^1(t) - p^2(t)\}.$$

Therefore by imposing that $p^1(0) = p^2(0)$, the function $t \mapsto |\Delta(t)|$ admits a stationary point at time $t = 0$. This is geometrically intuitive as the trajectories at time zero are parallel to one another for an infinitesimally small amount of time. To characterize this stationary point, we compute

$$\frac{1}{2} \frac{d^2}{dt^2} |\Delta(t)|^2 = -\Delta(t)^\top \{ \nabla U(q^1(t)) - \nabla U(q^2(t)) \} + |p^1(t) - p^2(t)|^2$$

and consider the following assumption.

Assumption 5 (Local convexity of potential). *There exists a compact set $S \in \mathcal{B}(\mathbb{R}^d)$, with positive Lebesgue measure, such that the restriction of U to S is α -strongly convex, i.e. there exists $\alpha > 0$ such that*

$$(q - q')^\top \{ \nabla U(q) - \nabla U(q') \} \geq \alpha |q - q'|^2$$

for all $q, q' \in S$.

Under Assumption 5, we have

$$\frac{1}{2} \frac{d^2}{dt^2} |\Delta(0)|^2 \leq -\alpha |\Delta(0)|^2 + |p^1(0) - p^2(0)|^2$$

if $q_0^1, q_0^2 \in S$ and $q_0^1 \neq q_0^2$. Therefore by taking $p^1(0) = p^2(0)$, it follows from the second derivative test that $t = 0$ is a strict local maximum point. Continuity of $t \mapsto |\Delta(t)|^2$ implies that there exists a trajectory length $T > 0$ such that for any $t \in (0, T]$, there exists $\rho \in [0, 1)$ satisfying

$$|\Phi_t^\circ(q_0^1, p_0) - \Phi_t^\circ(q_0^2, p_0)| \leq \rho |q_0^1 - q_0^2|. \quad (4)$$

We note the dependence of T on the initial positions q_0^1, q_0^2 and momentum p_0 . We now strengthen the above claim.

Lemma 1. *Suppose that the potential U satisfies Assumptions 4–5. For any compact set $A \subset S \times S \times \mathbb{R}^d$, there exists a trajectory length $T > 0$ such that for any $t \in (0, T]$, there exists $\rho \in [0, 1)$ satisfying (4) for all $(q_0^1, q_0^2, p_0) \in A$.*

It follows from the proof of Lemma 1 that the trajectory length T yielding contraction of the coupled system, and the corresponding contraction rate ρ associated to Φ_T° , do not depend on dimension d but only on the constants α and β . This suggests that such a coupling strategy can be effective in high dimension as long as the Hessian of U is sufficiently well-conditioned. See also [Mangoubi and Smith \[2017, Theorem 6\]](#) for a similar result.

3 Coupled Hamiltonian Monte Carlo

3.1 Leap-frog integrator

As the flow defined by (3) is typically intractable, one has to resort to time discretization. The leap-frog symplectic integrator is a standard choice as it preserves Properties 1 and 3. Given a step size $\varepsilon > 0$ and a number of leap-frog steps $L \in \mathbb{N}$, this scheme initializes at $(q_0, p_0) \in \mathbb{R}^d \times \mathbb{R}^d$ and iterates

$$p_{\ell+1/2} = p_\ell - \frac{\varepsilon}{2} \nabla U(q_\ell), \quad q_{\ell+1} = q_\ell + \varepsilon p_{\ell+1/2}, \quad p_{\ell+1} = p_{\ell+1/2} - \frac{\varepsilon}{2} \nabla U(q_{\ell+1}),$$

for $\ell = 0, \dots, L-1$. We write the leap-frog iteration as $\hat{\Phi}_\varepsilon(q_\ell, p_\ell) = (q_{\ell+1}, p_{\ell+1})$ and the corresponding approximation of the flow as $\hat{\Phi}_{\varepsilon, \ell}(q_0, p_0) = (q_\ell, p_\ell)$ for $\ell = 0, \dots, L$. As before, we denote by $\hat{\Phi}_{\varepsilon, \ell}^\circ(q_0, p_0) = q_\ell$ and $\hat{\Phi}_{\varepsilon, \ell}^*(q_0, p_0) = p_\ell$ the projections onto the position and momentum coordinates respectively.

Algorithm 1 Coupled Hamiltonian Monte Carlo step given (Q_{n-1}^1, Q_{n-1}^2) .

Sample momentum $P_n^* \sim \mathcal{N}(0_d, I_d)$ and $U_n \sim \mathcal{U}[0, 1]$ independently

For $i = 1, 2$

Set $(q_0^i, p_0^i) = (Q_{n-1}^i, P_n^*)$

Perform leap-frog integration to obtain $(q_L^i, p_L^i) = \hat{\Phi}_{\varepsilon, L}(q_0^i, p_0^i)$

If $U_n < \alpha\{(q_0^i, p_0^i), (q_L^i, p_L^i)\}$, set $(Q_n^i, P_n^i) = (q_L^i, -p_L^i)$

Otherwise set $(Q_n^i, P_n^i) = (Q_{n-1}^i, P_n^*)$

Under appropriate assumptions, it can be established that the leap-frog scheme is of order two [Hairer et al., 2005, Theorem 3.4], i.e. for sufficiently small ε , we have

$$|\hat{\Phi}_{\varepsilon, L}(q_0, p_0) - \Phi_{\varepsilon L}(q_0, p_0)| \leq C_4(q_0, p_0, L)\varepsilon^2, \quad (5)$$

$$|E\{\hat{\Phi}_{\varepsilon, L}(q_0, p_0)\} - E(q_0, p_0)| \leq C_5(q_0, p_0, L)\varepsilon^2, \quad (6)$$

for some positive constants C_4 and C_5 that depend continuously on the initial condition (q_0, p_0) for any number of leap-frog iterations L . We will assume throughout the article that (5) and (6) hold. While the constant associated to the pathwise error bound (5) will typically grow exponentially with L [Leimkuhler and Matthews, 2015, Section 2.2.3], the constant of the Hamiltonian error bound (6) on the other hand can be stable over exponentially long time intervals εL [Hairer et al., 2005, Theorem 8.1]. Although the Hamiltonian is not conserved exactly under time discretization, one can employ a Metropolis–Hastings correction as described in the following section.

3.2 Coupled Hamiltonian Monte Carlo kernel

Hamiltonian Monte Carlo [Duane et al., 1987, Neal, 1993] is a Metropolis–Hastings algorithm on phase space that targets $\tilde{\pi}$ using time discretized Hamiltonian dynamics as proposals. In view of Section 2.2, we consider coupling two Hamiltonian Monte Carlo chains $(Q_n^i, P_n^i)_{n \geq 0}$, $(i = 1, 2)$ by initializing $(Q_0^1, Q_0^2) \sim \tilde{\pi}_0$ and evolving the chains jointly according to Algorithm 1. Since the leap-frog integrator preserves Properties 1 and 3, the Metropolis–Hastings acceptance probability is

$$\alpha\{(q, p), (q', p')\} = \min [1, \exp\{E(q, p) - E(q', p')\}], \quad (7)$$

for $(q, p), (q', p') \in \mathbb{R}^d \times \mathbb{R}^d$. Iterating the above yields $\tilde{\pi}$ -invariant Markov chains $(Q_n^i, P_n^i)_{n \geq 0}$, $(i = 1, 2)$ on phase space, thus the marginal chains $(Q_n^i)_{n \geq 0}$, $(i = 1, 2)$ are π -invariant. Algorithm 1 amounts to running two Hamiltonian Monte Carlo chains with common random numbers; this has been considered in Neal [2002] to remove the burn-in bias and in Mangoubi and Smith [2017] to analyze mixing properties for strongly log-concave target distributions.

We denote the associated coupled Markov transition kernel on the position coordinates as $\bar{K}_{\varepsilon, L}((q^1, q^2), A^1 \times A^2)$ for $q^1, q^2 \in \mathbb{R}^d$ and $A^1, A^2 \in \mathcal{B}(\mathbb{R}^d)$. Marginally we have $\bar{K}_{\varepsilon, L}((q^1, q^2), A^1 \times \mathbb{R}^d) = K_{\varepsilon, L}(q^1, A^1)$ and $\bar{K}_{\varepsilon, L}((q^1, q^2), \mathbb{R}^d \times A^2) = K_{\varepsilon, L}(q^2, A^2)$, where $K_{\varepsilon, L}$ denotes the Markov transition kernel of the marginal Hamiltonian Monte Carlo chain. If we supplement Assumption 4 with the growth condition $|\nabla U(q)| \leq C_3(1 + |q|^{\kappa_3})$ for some $C_3 > 0$, $\kappa_3 \in [0, 1]$ and all $q \in \mathbb{R}^d$, aperiodicity, Lebesgue-irreducibility and Harris recurrence of $K_{\varepsilon, L}$ follow from Durmus et al. [2017, Theorem 2]; see also Cances et al. [2007] and Livingstone et al.

[2016] for previous works. Hence ergodicity follows from Meyn and Tweedie [2009, Theorem 13.0.1] and Assumption 1 is satisfied for test functions satisfying $\pi(h^{2+\kappa_1}) < \infty$ for some $\kappa_1 > 0$.

We will write the law of the coupled Hamiltonian Monte Carlo chain as $\mathbb{P}_{\varepsilon,L}$, and $\mathbb{E}_{\varepsilon,L}$ to denote expectation with respect to $\mathbb{P}_{\varepsilon,L}$. The following result establishes that the relaxed meeting time $\tau_\delta = \inf\{n \geq 0 : |Q_n^1 - Q_n^2| \leq \delta\}$, for any $\delta > 0$, has geometric tails.

Theorem 1. *Suppose that the potential U satisfies Assumptions 4–5. Assume also that there exists $\tilde{\varepsilon} > 0$ such that for any $\varepsilon \in (0, \tilde{\varepsilon})$ and $L \in \mathbb{N}$, there exist a measurable function $V : \mathbb{R}^d \rightarrow [1, \infty)$, $\lambda \in (0, 1)$ and $b < \infty$ such that*

$$K_{\varepsilon,L}(V)(q) \leq \lambda V(q) + b \quad (8)$$

for all $q \in \mathbb{R}^d$, $\pi_0(V) < \infty$ and $\{q \in \mathbb{R}^d : V(q) \leq \ell_1\} \subseteq \{q \in S : U(q) \leq \ell_0\}$ for some $\ell_0 \in (\inf_{q \in S} U(q), \sup_{q \in S} U(q))$ and $\ell_1 > 1$ satisfying $\lambda + 2b(1 - \lambda)^{-1}(1 + \ell_1)^{-1} < 1$. Then for any $\delta > 0$, there exist $\varepsilon_0 \in (0, \tilde{\varepsilon})$ and $L_0 \in \mathbb{N}$ such that for any $\varepsilon \in (0, \varepsilon_0)$ and $L \in \mathbb{N}$ satisfying $\varepsilon L < \varepsilon_0 L_0$, we have

$$\mathbb{P}_{\varepsilon,L}(\tau_\delta > n) \leq C_0 \kappa_0^n \quad (9)$$

for some $C_0 \in \mathbb{R}_+$, $\kappa_0 \in (0, 1)$ and all integer $n \geq 0$.

The proof of Theorem 1 proceeds by first showing that the relaxed meeting can take place, in finite iterations, whenever both chains enter a region of the state space where the target distribution is log-concave. As suggested in Neal [2002], one can expect good coupling behaviour if the chains spend enough time in this region of the state space; the second part of the proof makes this intuition precise by controlling excursions with the geometric drift condition (8). The latter can be established under additional assumptions on the potential U [Durmus et al., 2017, Theorem 9].

As Theorem 1 implies that the coupled chains can get arbitrarily close with sufficient frequency, one could potentially employ the unbiased estimation framework of Glynn and Rhee [2014] that introduces a truncation variable. To verify Assumption 2 that requires exact meetings, in the next section, we combine the coupled Hamiltonian Monte Carlo kernel with another coupled kernel that is designed to trigger exact meetings when the two chains are close.

4 Unbiased Hamiltonian Monte Carlo

4.1 Coupled random walk Metropolis–Hastings kernel

Let K_σ denote the π -invariant Gaussian random walk Metropolis–Hastings kernel with proposal covariance $\sigma^2 I_d$. The following describes a coupling of $K_\sigma(x, \cdot)$ and $K_\sigma(y, \cdot)$ that results in exact meetings with high probability when $x, y \in \mathbb{R}^d$ are close [Johnson, 1998, Jacob et al., 2017] and σ is appropriately chosen.

We begin by sampling the proposals $X^* \sim \mathcal{N}(x, \sigma^2 I_d)$ and $Y^* \sim \mathcal{N}(y, \sigma^2 I_d)$ from the maximal coupling of these two Gaussian distributions [Jacob et al., 2017, Section 4.1]. Under the maximal coupling, the probability that $\{X^* \neq Y^*\}$ is equal to the total variation distance between the distributions $\mathcal{N}(x, \sigma^2 I_d)$ and $\mathcal{N}(y, \sigma^2 I_d)$. Analytical tractability in the Gaussian case allows us to write that distance as $\mathbb{P}(2\sigma|Z| \leq \delta)$, where $Z \sim \mathcal{N}(0, 1)$ and $\delta = |x - y|$. By approximating the folded Gaussian cumulative distribution function [Pollard, 2005], we obtain

$$\mathbb{P}(X^* = Y^*) = \mathbb{P}(2\sigma|Z| > \delta) = 1 - (2\pi)^{-1/2} \frac{\delta}{\sigma} + \mathcal{O}\left(\frac{\delta^2}{\sigma^2}\right) \quad (10)$$

Algorithm 2 Compute unbiased estimator $H_{k:m}(X, Y)$ of $\pi(h)$

Initialize $(X_0, Y_0) \sim \bar{\pi}_0$ from a coupling with π_0 as marginals
With probability γ , sample $X_1 \sim K_\sigma(X_0, \cdot)$; otherwise sample $X_1 \sim K_{\varepsilon,L}(X_0, \cdot)$
Set $n = 1$. While $X_n \neq Y_{n-1}$ and $n < m$
 With probability γ , sample $(X_{n+1}, Y_n) \sim \bar{K}_\sigma((X_n, Y_{n-1}), \cdot)$
 Otherwise sample $(X_{n+1}, Y_n) \sim \bar{K}_{\varepsilon,L}((X_n, Y_{n-1}), \cdot)$
 If $X_{n+1} = Y_n$ set $\tau = n + 1$
 Increment $n \leftarrow n + 1$
Compute $H_{k:m}(X, Y)$ using (2)

as $\delta/\sigma \rightarrow 0$. Hence to achieve $\mathbb{P}(X^* = Y^*) = \theta$ for some desired probability θ , σ should be chosen approximately as $\delta/\{(2\pi)^{1/2} (1 - \theta)\}$.

The proposed values X^* and Y^* are then accepted according to Metropolis–Hastings acceptance probabilities, i.e. if $U^* \leq \min\{1, \pi(X^*)/\pi(x)\}$ and $U^* \leq \min\{1, \pi(Y^*)/\pi(y)\}$ respectively, where a common uniform random variable $U^* \sim \mathcal{U}[0, 1]$ is used for both chains. We denote the resulting coupled Markov transition kernel on $(\mathbb{R}^d \times \mathbb{R}^d, \mathcal{B}(\mathbb{R}^d) \times \mathcal{B}(\mathbb{R}^d))$ as \bar{K}_σ . If σ is small relative to the spread of the target distribution, the probability of accepting both proposals would be high. On the other hand, (10) shows that σ needs to be large compared to δ for the event $\{X^* = Y^*\}$ to occur with high probability. This leads to a trade-off; in practice, one can monitor the distance of coupled Hamiltonian Monte Carlo chains from preliminary runs to guide the choice of σ , as illustrated in Section 5.3.

4.2 Combining coupled kernels

We now combine the coupled Hamiltonian Monte Carlo kernel $\bar{K}_{\varepsilon,L}$ with the coupled random walk Metropolis–Hastings kernel \bar{K}_σ , introduced in Sections 3.2 and 4.1 respectively, using the following mixture

$$\bar{K}_{\varepsilon,L,\sigma}((x, y), A \times B) = (1 - \gamma)\bar{K}_{\varepsilon,L}((x, y), A \times B) + \gamma\bar{K}_\sigma((x, y), A \times B) \quad (11)$$

for $x, y \in \mathbb{R}^d$ and $A, B \in \mathcal{B}(\mathbb{R}^d)$, where $\gamma \in (0, 1), \varepsilon > 0, L \in \mathbb{N}, \sigma > 0$ are appropriately chosen. For the case $L = 1$, which reduces to the Metropolis-adjusted Langevin algorithm, an alternative to (11) can be constructed and is detailed in Appendix A. The rationale for the above choice is to enable exact meetings using the coupled random walk Metropolis–Hastings kernel when the chains are brought close together by the coupled Hamiltonian Monte Carlo kernel. We will write $Q_\sigma(x, A) = \int_A \mathcal{N}(y; x, \sigma^2 I_d) dy, x \in \mathbb{R}^d, A \in \mathcal{B}(\mathbb{R}^d)$ as the Markov transition kernel of the Gaussian random walk, the law of the resulting coupled chain $(X_n, Y_n)_{n \geq 0}$ as $\mathbb{P}_{\varepsilon,L,\sigma}$, and $\mathbb{E}_{\varepsilon,L,\sigma}$ to denote expectation with respect to $\mathbb{P}_{\varepsilon,L,\sigma}$. Algorithm 2 details the use of $(X_n, Y_n)_{n \geq 0}$ to compute the unbiased estimators described in Section 1.3.

The mixture kernel $K_{\varepsilon,L,\sigma} = (1 - \gamma)K_{\varepsilon,L} + \gamma K_\sigma$ inherits ergodicity properties from any of its components, therefore Assumption 1 can be satisfied following the discussion in Section 3.2. Noting that the faithfulness property in Assumption 3 holds by construction, we now turn our attention to Assumption 2.

Theorem 2. *Suppose that the potential U satisfies Assumptions 4–5. Assume also that there exist $\tilde{\varepsilon} > 0$ and $\tilde{\sigma} > 0$ such that for any $\varepsilon \in (0, \tilde{\varepsilon}), L \in \mathbb{N}$ and $\sigma \in (0, \tilde{\sigma})$, there exist a measurable function $V : \mathbb{R}^d \rightarrow [1, \infty)$, $\lambda \in (0, 1), b < \infty$ and $\mu > 0$ such that*

$$K_{\varepsilon,L}(V)(x) \leq \lambda V(x) + b \quad \text{and} \quad Q_\sigma(V)(x) \leq \mu\{V(x) + 1\} \quad (12)$$

for all $x \in \mathbb{R}^d$, $\pi_0(V) < \infty$, $\lambda_0 = (1 - \gamma)\lambda + \gamma(1 + \mu) < 1$ and $\{x \in \mathbb{R}^d : V(x) \leq \ell_1\} \subseteq \{x \in S : U(x) \leq \ell_0\}$ for some $\ell_0 \in (\inf_{x \in S} U(x), \sup_{x \in S} U(x))$ and $\ell_1 > 1$ satisfying $\lambda_0 + 2\{(1 - \gamma)b + \gamma\mu\}(1 - \lambda_0)^{-1}(1 + \ell_1)^{-1} < 1$. Then there exist $\varepsilon_0 \in (0, \tilde{\varepsilon})$, $L_0 \in \mathbb{N}$ and $\sigma_0 > 0$ such that for any $\varepsilon \in (0, \varepsilon_0)$, $L \in \mathbb{N}$ satisfying $\varepsilon L < \varepsilon_0 L_0$ and $\sigma \in (0, \sigma_0)$, we have

$$\mathbb{P}_{\varepsilon, L, \sigma}(\tau > n) \leq C_0 \kappa_0^n \quad (13)$$

for some $C_0 \in \mathbb{R}_+$, $\kappa_0 \in (0, 1)$ and all integer $n \geq 0$.

Proof of the above result proceeds in two parts as in Theorem 1, but requires slightly stronger assumptions to ensure that the mixture kernel still satisfies a geometric drift condition. The additional assumption in (12) can be verified when the form of V is known, and is satisfied for example by the Lyapunov function employed in Durmus et al. [2017, Theorem 9]. Although the above discussion guarantees validity of the unbiased estimator computed by Algorithm 2 for a range of tuning parameters, its efficiency will depend on the distribution of the meeting time τ induced by the coupling and mixing properties of the marginal kernel $K_{\varepsilon, L, \sigma}$. We will illustrate in Section 5 that tuning parameters that are optimal for the marginal Hamiltonian Monte Carlo kernel $K_{\varepsilon, L}$ might not necessarily be adequate for our purposes.

5 Numerical illustrations

5.1 Preliminaries

In practice, we will run Algorithm 2 R times independently in parallel to obtain the unbiased estimators $H_{k:m}^{(r)}(X, Y)$, $r = 1, \dots, R$. Following the framework of Glynn and Whitt [1992], we define the asymptotic inefficiency in the limit of our computational budget as

$$i(h, \bar{\pi}_0, \bar{K}_{\varepsilon, L, \sigma}) = \mathbb{E}_{\varepsilon, L, \sigma} [2\tau + \max(1, m + 1 - \tau)] \text{Var}_{\varepsilon, L, \sigma} [H_{k:m}(X, Y)],$$

assuming that applying $\bar{K}_{\varepsilon, L, \sigma}$ costs twice as much as $K_{\varepsilon, L, \sigma}$. This accounts for the fact that, with a given compute budget, one can average over more estimators if each is cheaper to compute. We will approximate this asymptotic inefficiency by empirical averages over the R realizations. For comparison, the asymptotic variance of a standard Hamiltonian Monte Carlo estimator, defined as

$$v(h, K_{\varepsilon, L}) = \lim_{n \rightarrow \infty} \text{Var}_{\varepsilon, L} \left[n^{-1/2} \sum_{i=1}^n h(X_i) \right]$$

where $X_0 \sim \pi$ and $X_n \sim K_{\varepsilon, L}(X_{n-1}, \cdot)$ for all integer $n \geq 1$, will be approximated with the `spectrum0.ar` function of the `coda` R package [Plummer et al., 2006] using 10,000 iterations after a burn-in of 1,000 for all examples. We will consider estimating first and second moments, i.e. set $h_i(x) = x_i$ and $h_{d+i}(x) = x_i^2$ for $i = 1, \dots, d$, and compare $i(\bar{\pi}_0, \bar{K}_{\varepsilon, L, \sigma}) = \sum_{i=1}^{2d} i(h_i, \bar{\pi}_0, \bar{K}_{\varepsilon, L, \sigma})$ with $v(K_{\varepsilon, L}) = \sum_{i=1}^{2d} v(h_i, K_{\varepsilon, L})$ at possibly different parameter configurations. An important point to be illustrated in the following is that the parameters ε and L minimizing the asymptotic inefficiency $Lv(K_{\varepsilon, L})$, assuming that leap-frog iterations dominate the cost of $K_{\varepsilon, L}$, might not necessarily be suitable for our proposed estimator. Lastly, we will employ the guideline of taking k as the 90% sample quantile of meeting times, obtained from a small number of preliminary runs, and setting $m = 10k$.

5.2 Truncated Gaussian distribution

We first investigate coupling Hamiltonian Monte Carlo on truncated Gaussian distributions constrained by quadratic inequalities. Pakman and Paninski [2014] introduced an algorithm that generates trajectories

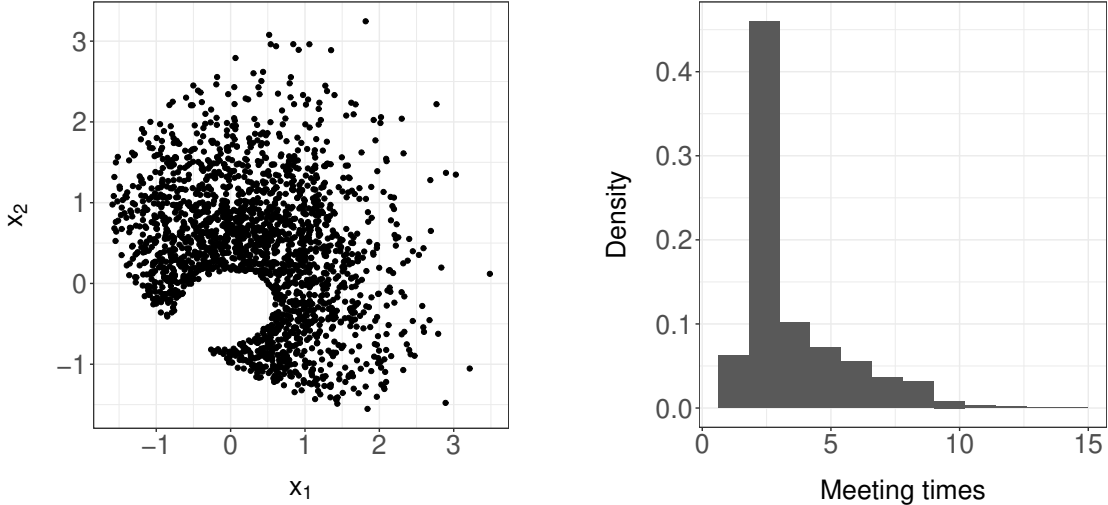


Figure 1: Truncated Gaussian example in Section 5.2. (Left) Scatter plot of 2,000 Hamiltonian Monte Carlo samples approximating a Gaussian distribution truncated by quadratic constraints. (Right) Histogram of relaxed meeting times for 1,000 coupled Hamiltonian Monte Carlo chains.

which undergo exact Hamiltonian dynamics and bounce off the constraints. Implementing our method only involved simple modifications of their `tmg` R package [Pakman, 2012].

Following Pakman and Paninski [2014], we consider a bivariate standard Gaussian distribution restricted to the set $\{(x_1, x_2) \in \mathbb{R}^2 : (x_1 - 4)^2/32 + (x_2 - 1)^2/8 \leq 1, 4x_1^2 + 8x_2^2 - 2x_1x_2 + 5x_2 \geq 1\}$ and use $\pi/2$ as the trajectory length advocated therein. The left panel of Figure 1 displays 2,000 Hamiltonian Monte Carlo samples. Setting $(2, 0)$ as the initial position of both chains, the coupling proposed in Section 2.2 yields rapidly contracting chains that are within machine precision in a few iterations. A histogram of relaxed meeting times, with respect to machine precision, is shown in the right panel of Figure 1. Our guideline for the choice of k and m yields $k = 6$ and $m = 60$, based on 100 draws of meeting times. With these values, we computed $R = 1,000$ unbiased estimators and obtained an approximate asymptotic inefficiency of 7.15. In this case, the loss of efficiency is insignificant compared to the Hamiltonian Monte Carlo algorithm, for which the asymptotic variance was found to be approximately 6.41.

5.3 Logistic regression

We now consider a Bayesian logistic regression on the classic German credit dataset, as in Hoffman and Gelman [2014]. After including all pairwise interactions and performing standardization, the design matrix has 1,000 rows and 300 columns. Given covariates $x_i \in \mathbb{R}^{300}$, intercept $a \in \mathbb{R}$ and coefficients $b \in \mathbb{R}^{300}$, each observation $y_i \in \{0, 1\}$ is modelled as an independent Bernoulli random variable with probability of success $\{1 + \exp(-a - b^\top x_i)\}^{-1}$. The prior is specified as $a|s^2 \sim \mathcal{N}(0, s^2)$, $b|s^2 \sim \mathcal{N}(0_{300}, s^2 I_{300})$ independently, and an Exponential distribution with rate 0.01 for the variance parameter s^2 . The target π is the posterior distribution of parameters $(a, b, \log s^2)$ on \mathbb{R}^d with $d = 302$.

Initializing coupled chains independently from $\pi_0 = \mathcal{N}(0_d, I_d)$, for each parameter configuration $(\varepsilon, L) \in \{0.01, 0.0125, \dots, 0.04\} \times \{10, 20, 30\}$, we run 5 pairs of coupled Hamiltonian Monte Carlo chains for 1,000 iterations. This computation can be done independently in parallel for each configuration and repeat; the

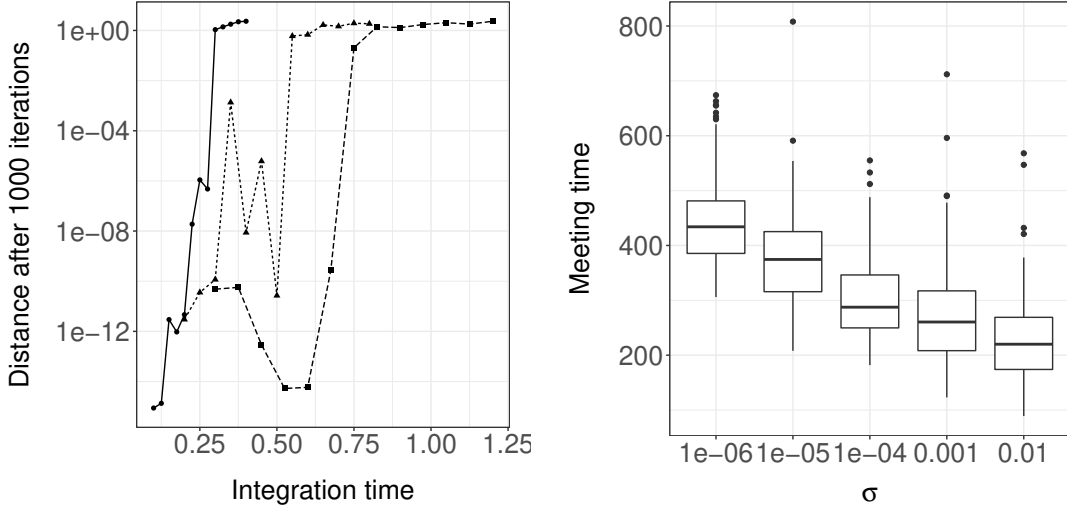


Figure 2: Logistic regression example in Section 5.3. (Left) Average distance between coupled chains at iteration 1,000 against integration time εL . The symbols and lines correspond to $L = 10$ (dot-solid), $L = 20$ (triangle-small dashes) and $L = 30$ (square-dashes). (Right) Boxplot of meeting times as parameter σ varies.

output is displayed in the left panel of Figure 2. Although multiple configurations lead to contractive chains, it is not the case for $(\varepsilon, L) = (0.03, 10)$ which are optimal parameters for Hamiltonian Monte Carlo. For configurations that yield distances that are less than 10^{-10} , we simulate 100 meeting times in parallel using the mixture kernel (11) with $\gamma = 1/20$ and $\sigma = 10^{-3}$. We then select the parameter configuration $(\varepsilon, L) = (0.0125, 10)$ that gave the least average compute cost, taken as L times the average meeting time.

To illustrate the impact of σ , in the right panel of Figure 2, we fix $(\varepsilon, L) = (0.0125, 10)$ and examine the distribution of meeting times as σ varies. Decreasing σ leads to larger meeting times: conservatively small values of σ require more iterations before the chains get close enough for the maximal coupling to propose the same value with high probability. On the other hand, if σ was too large, large meeting times would be observed as random walk proposals would be rejected with high probability. The figure suggests that the effectiveness of our coupling is not highly sensitive to the choice of σ , provided that it is small enough.

Finally, we produce $R = 1,000$ coupled chains in parallel with $(\varepsilon, L, \sigma) = (0.0125, L = 10, 10^{-3})$ and compare the inefficiency of our estimator with the asymptotic variance of the optimal Hamiltonian Monte Carlo estimator for various choices of k and m . The results, summarized in Table 1, illustrate that bias removal comes at a cost of increased variance, and that this can be reduced with appropriate choices of k and m . Our guideline for k and m results in a relative inefficiency of 1.05 at an average compute cost of 3518 applications of $K_{\varepsilon, L, \sigma}$, or approximately 5 minutes of computing time with our implementation. Thanks to unbiasedness, we can safely average over independent copies of an estimator whose expected cost is of the order of a few thousand Hamiltonian Monte Carlo iterations.

5.4 Log-Gaussian Cox point processes

We end with a challenging high dimensional application of Bayesian inference for log-Gaussian Cox point processes on a dataset concerning the locations of 126 Scot pine saplings in a natural forest in Finland [Møller et al., 1998]. After discretizing the plot into a 64×64 regular grid, the number of points in each grid

Table 1: Relative inefficiency of proposed estimator in logistic regression example

k	m	Cost	Variance	Relative inefficiency
1	k	436	4.0×10^2	1989.07
1	$5k$	436	3.4×10^2	1671.93
1	$10k$	436	2.8×10^2	1403.28
median(τ)	k	458	7.4×10^0	38.22
median(τ)	$5k$	1258	1.1×10^{-1}	1.58
median(τ)	$10k$	2298	4.5×10^{-2}	1.18
90% quantile(τ)	k	553	6.0×10^0	38.11
90% quantile(τ)	$5k$	1868	5.8×10^{-2}	1.23
90% quantile(τ)	$10k$	3518	2.6×10^{-2}	1.05

Table 2: Cost refers to the expected compute cost, variance denotes the sum of variances when estimating first and second moments, and relative inefficiency is the ratio of the asymptotic inefficiency $i(\bar{\pi}_0, \bar{K}_{\varepsilon, L, \sigma})$ with parameters $(\varepsilon, L, \sigma) = (0.0125, 10, 10^{-3})$, to the asymptotic variance $v(K_{\varepsilon, L})$ with optimal parameters $(\varepsilon, L) = (0.03, 10)$. These quantities were computed using $R = 1,000$ independent runs, while the median and 90% quantile of the meeting time were computed with 100 preliminary runs.

cell $y_i \in \mathbb{N}$ is assumed to be conditionally independent, given a latent intensity process $\Lambda_i, i \in \{1, \dots, 64\}^2$, and modelled as Poisson distributed with mean $a\Lambda_i$, where $a = 1/4096$ is the area of each grid cell. The prior is specified by $\Lambda_i = \exp(X_i)$, where $X_i, i \in \{1, \dots, 64\}^2$ is a Gaussian process with mean $\mu \in \mathbb{R}$ and exponential covariance function $\Sigma_{i,j} = s^2 \exp\{-|i-j|/(64b)\}$ for $i, j \in \{1, \dots, 64\}^2$. We will adopt the parameter values $s^2 = 1.91, b = 1/33$ and $\mu = \log(126) - s^2/2$ estimated by [Møller et al. \[1998\]](#) and infer the posterior distribution of the latent process $X_i, i \in \{1, \dots, 64\}^2$ given the count data and these hyperparameter values. This corresponds to a target distribution π on \mathbb{R}^d with $d = 4096$.

Owing to the high dimensionality of this model, the mixing of random walk Metropolis–Hastings is known to be prohibitively slow [[Christensen and Waagepetersen, 2002](#)], while the Metropolis-adjusted Langevin algorithm requires a computationally costly reparameterization to be effective [[Christensen et al., 2005](#)]. We will consider the use of Hamiltonian Monte Carlo and Riemann manifold Hamiltonian Monte Carlo with metric tensor $\Sigma^{-1} + a \exp(\mu + s^2/2) I_d$ [[Girolami and Calderhead, 2011](#)]. We proceed as in Section 5.3 to seek parameter configurations $(\varepsilon, L) \in \{0.05, 0.07, \dots, 0.45\} \times \{10, 20, 30\}$ that yield contractive coupled chains with small compute cost, when initialized independently from the prior distribution. Although both algorithms have multiple configurations that result in contractive chains, the parameters $(\varepsilon, L) = (0.25, 10)$, which were optimal for both methods, only led to contractive coupled Riemann manifold Hamiltonian Monte Carlo chains. By simulating 100 meeting times with $\gamma = 1/20$ and $\sigma = 10^{-3}$ for configurations that yield distances of less than 10^{-10} , we select $(\varepsilon, L) = (0.17, 10)$ for Hamiltonian Monte Carlo and $(\varepsilon, L) = (0.13, 10)$ for Riemann manifold Hamiltonian Monte Carlo, which gave the smallest average compute cost for each algorithm. The corresponding meeting times in the left panel of Figure 3 show the effectiveness of our coupling strategy even in high dimensions.

With these parameters and the guideline for choosing k and m , we computed $R = 1,000$ coupled chains in parallel for each algorithm. The estimated posterior mean of the latent process is displayed in the right panel of Figure 3. The relative inefficiency was found to be 2.73 and 3.72 for Hamiltonian Monte Carlo and Riemann

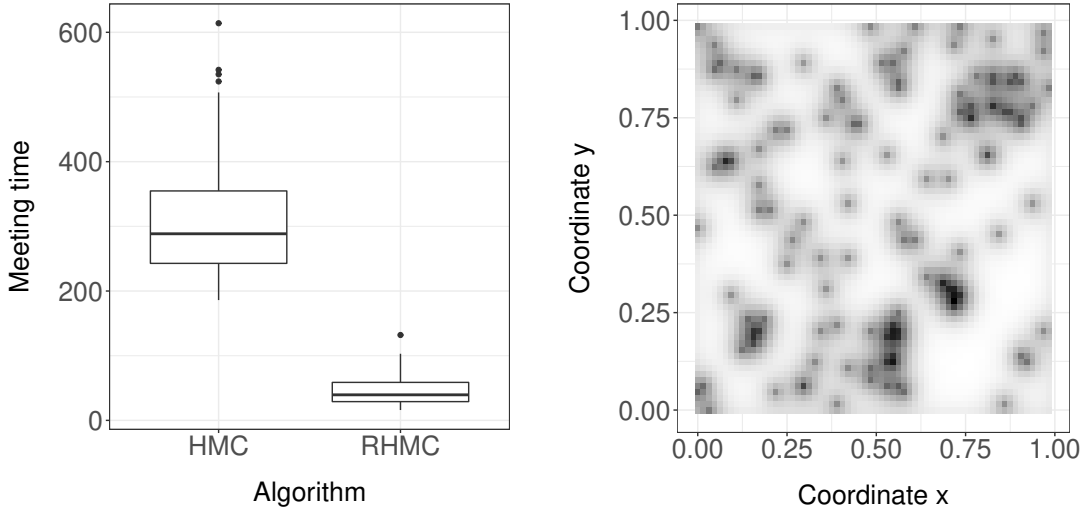


Figure 3: Cox process example in Section 5.4. (Left) Boxplot of meeting times for both algorithms. (Right) Estimated posterior mean of latent process.

manifold Hamiltonian Monte Carlo respectively, and the corresponding compute time was approximately 90 and 20 minutes with our implementation. Despite some loss of efficiency, the benefits of exploiting parallel computation for this problem is apparent since one can only run 4439 and 714 iterations of these algorithms respectively for the same compute time.

6 Discussion

Construction of couplings could be explored for other variants of the Hamiltonian Monte Carlo method, such as the use of partial momentum refreshment [Horowitz, 1991], the adaptation of tuning parameters [Hoffman and Gelman, 2014], different choices of kinetic energy [Livingstone et al., 2017], and in combination with new sampling paradigms [Pollock et al., 2016, Fearnhead et al., 2016, Vanetti et al., 2017]. Other ways of leveraging parallel hardware for Hamiltonian Monte Carlo include the work in Calderhead [2014], which builds on Tjelmeland [2004], that focuses on parallel computation at each iteration of the algorithm.

Acknowledgement

The computations in this article were run on the Odyssey cluster supported by the FAS Division of Science, Research Computing Group at Harvard University. Pierre E. Jacob gratefully acknowledges support by the National Science Foundation through grant DMS-1712872.

References

- A. Beskos, N. Pillai, G. Roberts, J.-M. Sanz-Serna, and A. Stuart. Optimal tuning of the Hybrid Monte Carlo algorithm. *Bernoulli*, 19(5A):1501–1534, 2013. 1
- M. Betancourt. A conceptual introduction to Hamiltonian Monte Carlo. *arXiv preprint arXiv:1701.02434*, 2017. 1

M. Betancourt, S. Byrne, S. Livingstone, and M. Girolami. The geometric foundations of Hamiltonian Monte Carlo. *Bernoulli*, 23(4A):2257–2298, 2017. [1](#)

S. P. Brooks, A. Gelman, G. Jones, and X.-L. Meng. *Handbook of Markov chain Monte Carlo*. CRC press, 2011. [1](#)

B. Calderhead. A general construction for parallelizing Metropolis–Hastings algorithms. *Proceedings of the National Academy of Sciences*, 111(49):17408–17413, 2014. [13](#)

E. Cancès, F. Legoll, and G. Stoltz. Theoretical and numerical comparison of some sampling methods for molecular dynamics. *ESAIM: Mathematical Modelling and Numerical Analysis*, 41(2):351–389, 2007. [6](#)

B. Carpenter, A. Gelman, M. D. Hoffman, D. Lee, B. Goodrich, M. Betancourt, M. A. Brubaker, J. Guo, P. Li, and A. Riddell. Stan: a probabilistic programming language. *Journal of Statistical Software*, 20: 1–37, 2016. [1](#)

G. Casella, M. Lavine, and C. P. Robert. Explaining the perfect sampler. *The American Statistician*, 55(4): 299–305, 2001. [1](#)

O. F. Christensen and R. Waagepetersen. Bayesian prediction of spatial count data using generalized linear mixed models. *Biometrics*, 58(2):280–286, 2002. [12](#)

O. F. Christensen, G. O. Roberts, and J. S. Rosenthal. Scaling limits for the transient phase of local Metropolis–Hastings algorithms. *J. Royal Statist. Society Series B*, 67(2):253–268, 2005. [12](#)

A. Dalalyan. Further and stronger analogy between sampling and optimization: Langevin Monte Carlo and gradient descent. In *Proceedings of the 2017 Conference on Learning Theory*, volume 65 of *Proceedings of Machine Learning Research*, pages 678–689. PMLR, 07–10 Jul 2017. URL <http://proceedings.mlr.press/v65/dalalyan17a.html>. [15](#)

S. Duane, A. D. Kennedy, B. J. Pendleton, and D. Roweth. Hybrid Monte Carlo. *Physics Letters B*, 195(2): 216–222, 1987. [1, 6](#)

A. Durmus, E. Moulines, and E. Saksman. On the convergence of Hamiltonian Monte Carlo. *arXiv preprint arXiv:1705.00166*, 2017. [6, 7, 9](#)

P. Fearnhead, J. Bierkens, M. Pollock, and G. O. Roberts. Piecewise deterministic Markov processes for continuous-time Monte Carlo. *arXiv preprint arXiv:1611.07873*, 2016. [13](#)

M. Girolami and B. Calderhead. Riemann manifold Langevin and Hamiltonian Monte Carlo methods. *J. Royal Statist. Society Series B*, 73(2):123–214, 2011. [1, 12](#)

P. W. Glynn and C.-H. Rhee. Exact estimation for Markov chain equilibrium expectations. *Journal of Applied Probability*, 51(A):377–389, 2014. [1, 2, 7](#)

P. W. Glynn and W. Whitt. The asymptotic efficiency of simulation estimators. *Operations Research*, 40(3): 505–520, 1992. [3, 9](#)

E. Hairer, G. Wanner, and C. Lubich. *Geometric numerical integration: structure-preserving algorithms for ordinary differential equations*. Springer-Verlag, New York, 2005. [6](#)

M. D. Hoffman and A. Gelman. The No-U-Turn Sampler: adaptively setting path lengths in Hamiltonian Monte Carlo. *Journal of Machine Learning Research*, 15(1):1593–1623, 2014. [1, 10, 13](#)

A. M. Horowitz. A generalized guided Monte Carlo algorithm. *Physics Letters B*, 268(2):247–252, 1991. [13](#)

M. Huber. *Perfect simulation*, volume 148. CRC Press, 2016. [1](#)

P. E. Jacob, J. O’Leary, and Y. F. Atchadé. Unbiased Markov chain Monte Carlo with couplings. *arXiv preprint arXiv:1708.03625v2*, 2017. [1, 2, 3, 7, 18](#)

V. E. Johnson. A coupling-regeneration scheme for diagnosing convergence in Markov chain Monte Carlo algorithms. *J. American Statist. Assoc.*, 93(441):238–248, 1998. [7](#)

B. Leimkuhler and C. Matthews. *Molecular Dynamics*. Springer-Verlag, New York, 2015. [6](#)

T. Lelièvre, M. Rousset, and G. Stoltz. *Free Energy Computations: A Mathematical Perspective*. Imperial College Press, 2010. ISBN 978-1-84816-248-8. [1](#), [4](#)

S. Livingstone, M. Betancourt, S. Byrne, and M. Girolami. On the geometric ergodicity of Hamiltonian Monte Carlo. *arXiv preprint arXiv:1601.08057*, 2016. [6](#)

S. Livingstone, M. F. Faulkner, and G. O. Roberts. Kinetic energy choice in Hamiltonian/hybrid Monte Carlo. *arXiv preprint arXiv:1706.02649*, 2017. [13](#)

O. Mangoubi and A. Smith. Rapid mixing of Hamiltonian Monte Carlo on strongly log-concave distributions. *arXiv preprint arXiv:1708.07114*, 2017. [1](#), [5](#), [6](#)

S. Meyn and R. Tweedie. *Markov chains and stochastic stability*. Cambridge University Press, 2nd edition, 2009. [7](#)

J. Møller, A. R. Syversveen, and R. P. Waagepetersen. Log Gaussian Cox processes. *Scandinavian Journal of Statistics*, 25(3):451–482, 1998. [11](#), [12](#)

P. Mykland, L. Tierney, and B. Yu. Regeneration in Markov chain samplers. *J. American Statist. Assoc.*, 90(429):233–241, 1995. [1](#)

R. M. Neal. Bayesian learning via stochastic dynamics. Advances in neural information processing systems, pages 475–475, 1993. [1](#), [6](#)

R. M. Neal. Circularly-coupled Markov chain sampling. *arXiv preprint arXiv:1711.04399*, 2002. [1](#), [6](#), [7](#)

A. Pakman. tmg: truncated multivariate Gaussian sampling. *CRAN*, 2012. URL <https://cran.r-project.org/package=tmg>. [10](#)

A. Pakman and L. Paninski. Exact Hamiltonian Monte Carlo for truncated multivariate Gaussians. *Journal of Computational and Graphical Statistics*, 23(2):518–542, 2014. [9](#), [10](#)

M. Plummer, N. Best, K. Cowles, and K. Vines. CODA: Convergence diagnosis and output analysis for MCMC. *R News*, 6(1):7–11, 2006. URL <https://journal.r-project.org/archive/>. [9](#)

D. Pollard. *Chapter 3: Total variation distance between measures*. Asymptopia, 2005. URL <http://www.stat.yale.edu/~pollard/Courses/607.spring05/handouts/Totalvar.pdf>. [7](#)

M. Pollock, P. Fearnhead, A. M. Johansen, and G. O. Roberts. The scalable Langevin exact algorithm: Bayesian inference for big data. *arXiv preprint arXiv:1609.03436*, 2016. [13](#)

J. S. Rosenthal. Faithful couplings of Markov chains: now equals forever. *Advances in Applied Mathematics*, 18(3):372–381, 1997. ISSN 0196-8858. [2](#)

J. S. Rosenthal. Parallel computing and Monte Carlo algorithms. *Far East Journal of Theoretical Statistics*, 4(2):207–236, 2000. [1](#)

H. Tjelmeland. Using all Metropolis–Hastings proposals to estimate mean values. Technical report, Department of Mathematical Sciences, Norwegian University of Science and Technology, 2004. [13](#)

P. Vanetti, A. Bouchard-Côté, G. Deligiannidis, and A. Doucet. Piecewise deterministic Markov chain Monte Carlo. *arXiv preprint arXiv:1707.05296*, 2017. [13](#)

A Coupling Metropolis-adjusted Langevin algorithm

We present an alternative to the construction in (11) for the case $L = 1$, which reduces to the Metropolis-adjusted Langevin algorithm with step size $\varepsilon > 0$. In this case, the coupled Hamiltonian Monte Carlo kernel $\bar{K}_{\varepsilon,1}$, introduced in Section 3, corresponds to a synchronous coupling of the proposal transition kernel $Q_\varepsilon(x, A) = \int_A \mathcal{N}(y; x + \nabla \log \pi(x)/2, \varepsilon^2 I_d) dy$, $x \in \mathbb{R}^d$, $A \in \mathcal{B}(\mathbb{R}^d)$, associated to the Euler–Maruyama discretization of a π -invariant Langevin diffusion on \mathbb{R}^d [Dalalyan, 2017].

To construct a coupling of $K_{\varepsilon,1}(x, \cdot)$ and $K_{\varepsilon,1}(y, \cdot)$ that prompts exact meetings when $x, y \in \mathbb{R}^d$ are close, we can sample the proposals (X^*, Y^*) from the maximal coupling of $Q_\varepsilon(x, \cdot)$ and $Q_\varepsilon(y, \cdot)$. Writing $\delta = |x - y|$, it follows from Assumption 4 and the approximation in (10) that

$$\mathbb{P}(X^* = Y^*) \geq 1 - \frac{(2 + \beta)}{2(2\pi)^{1/2}} \frac{\delta}{\varepsilon} + \mathcal{O}\left(\frac{\delta^2}{\varepsilon^2}\right)$$

as $\delta/\varepsilon \rightarrow 0$. As in Section 4.1, the proposed values are then accepted with Metropolis–Hastings acceptance probabilities with a common uniform random variable for both chains. We denote the resulting coupled Markov transition kernel on $(\mathbb{R}^d \times \mathbb{R}^d, \mathcal{B}(\mathbb{R}^d) \times \mathcal{B}(\mathbb{R}^d))$ as \bar{K}_ε . For some pre-specified threshold $\delta_0 > 0$, we can combine these coupled kernels by considering

$$\bar{K}((x, y), A \times B) = \mathbb{I}_{D_{\delta_0}^c}(x, y) \bar{K}_{\varepsilon,1}((x, y), A \times B) + \mathbb{I}_{D_{\delta_0}}(x, y) \bar{K}_\varepsilon((x, y), A \times B)$$

for $x, y \in \mathbb{R}^d$ and $A, B \in \mathcal{B}(\mathbb{R}^d)$, where $D_{\delta_0} = \{(x, y) \in \mathbb{R}^d \times \mathbb{R}^d : |x - y| \leq \delta_0\}$ and $D_{\delta_0}^c = \mathbb{R}^d \times \mathbb{R}^d \setminus D_{\delta_0}$. This coupled kernel admits the marginal Metropolis-adjusted Langevin algorithm kernel $K_{\varepsilon,1}$ as marginals, i.e. $\bar{K}((x, y), A \times \mathbb{R}^d) = K_{\varepsilon,1}(x, A)$ and $\bar{K}((x, y), \mathbb{R}^d \times A) = K_{\varepsilon,1}(y, A)$ for all $x, y \in \mathbb{R}^d$ and $A \in \mathcal{B}(\mathbb{R}^d)$, as this holds for both $\bar{K}_{\varepsilon,1}$ and \bar{K}_ε .

B Intermediate results

Proof of Lemma 1. Take $(q_0^1, q_0^2, p_0) \in A$. Applying Taylor's theorem on $\Delta(t)$ around $t = 0$ gives

$$\Delta(t) = \Delta(0) - \frac{1}{2}t^2 G_0 - \frac{1}{6}t^3 G_*$$

for some $t_* \in (0, t)$, where $G_0 = \nabla U(q_0^1) - \nabla U(q_0^2)$ and

$$G_* = \nabla^2 U\{q^1(t_*)\}p^1(t_*) - \nabla^2 U\{q^2(t_*)\}p^2(t_*).$$

We will control each term of the expansion

$$|\Delta(t)|^2 = |\Delta(0)|^2 - t^2 \Delta(0)^\top G_0 - \frac{1}{3}t^3 \Delta(0)^\top G_* + \frac{1}{4}t^4 |G_0|^2 + \frac{1}{6}t^5 G_0^\top G_* + \frac{1}{36}t^6 |G_*|^2.$$

Using strong convexity, the Lipschitz assumption and Young's inequality

$$|\Delta(t)|^2 \leq \left(1 - \alpha t^2 + \frac{1}{6}t^3 + \frac{1}{4}\beta^2 t^4 + \frac{1}{12}\beta^2 t^5\right) |\Delta(0)|^2 + \left(\frac{1}{6}t^3 + \frac{1}{12}t^5 + \frac{1}{36}t^6\right) |G_*|^2.$$

By Young's inequality and the Lipschitz assumption

$$\begin{aligned} |G_*|^2 &\leq 2\|\nabla^2 U\{q^1(t_*)\}\|_2^2 |p^1(t_*)|^2 + 2\|\nabla^2 U\{q^2(t_*)\}\|_2^2 |p^2(t_*)|^2 \\ &\leq 2\beta^2 \{|\Phi_{t_*}^*(q_0^1, p_0)|^2 + |\Phi_{t_*}^*(q_0^2, p_0)|^2\} \\ &\leq 2\beta^2 \sup_{(q_0^1, q_0^2, p_0) \in A} \{|\Phi_{t_*}^*(q_0^1, p_0)|^2 + |\Phi_{t_*}^*(q_0^2, p_0)|^2\} \end{aligned}$$

where $\|\cdot\|_2$ denotes the spectral norm. The above supremum is attained by continuity of the mapping $(q, p) \mapsto \Phi_{t_*}^*(q, p)$. The claim (4) follows by combining both inequalities and taking t sufficiently small. \square

To prove Theorem 1, we first establish the following intermediate result. For any measurable function $f : \Omega \rightarrow \mathbb{R}$ and subset $A \subseteq \Omega$, we will write its level sets as $L_\ell(f) = \{x \in \Omega : f(x) \leq \ell\}$ for $\ell \in \mathbb{R}$ and its restriction to A as $f_A : A \rightarrow \mathbb{R}$.

Proposition 1. Suppose that the potential U satisfies Assumptions 4–5. Then for any $\delta > 0$, $u_0 > \inf_{q \in S} U(q)$ and $u_1 < \sup_{q \in S} U(q)$ with $u_0 < u_1$, there exist $\bar{\varepsilon} > 0$ and $\bar{L} \in \mathbb{N}$ such that for any $\varepsilon \in (0, \bar{\varepsilon})$ and $L \in \mathbb{N}$ satisfying $\varepsilon L < \bar{\varepsilon} \bar{L}$, there exist $v_0 \in (u_0, u_1)$, $n_0 \in \mathbb{N}$ and $\omega \in (0, 1)$ such that

$$\inf_{q^1, q^2 \in S_0} \bar{K}_{\varepsilon, L}^{n_0} \{(q^1, q^2), D_\delta\} \geq \omega, \quad (14)$$

where $S_0 = L_{v_0}(U_S)$ is compact with positive Lebesgue measure,

$$\bar{K}_{\varepsilon, L}^n \{(q^1, q^2), A^1 \times A^2\} = \mathbb{P}_{\varepsilon, L} \{(Q_n^1, Q_n^2) \in A^1 \times A^2 \mid (Q_0^1, Q_0^2) = (q^1, q^2)\}$$

denotes the n -step transition probabilities of the coupled chain, and $D_\delta = \{(q, q') \in \mathbb{R}^d \times \mathbb{R}^d : |q - q'| \leq \delta\}$.

Proof of Proposition 1. Suppose that the chains $(Q_n^1)_{n \geq 0}, (Q_n^2)_{n \geq 0}$ are initialized at $Q_0^1 = q^1 \in S$ and $Q_0^2 = q^2 \in S$. Let $K(p) = |p|^2/2$ denote the kinetic energy function. By compactness of $A = S \times S \times L_{k_0}(K)$, for some $k_0 > 0$ to be specified, it follows from Lemma 1 that there exists a trajectory length $T > 0$ such that for any $t \in (0, T]$, there exists $\rho_0 \in [0, 1)$ satisfying

$$|\Phi_t^\circ(Q_0^1, P_1^*) - \Phi_t^\circ(Q_0^2, P_1^*)| \leq \rho_0 |Q_0^1 - Q_0^2|$$

for all $(Q_0^1, Q_0^2, P_1^*) \in A$. Hence there exists $\omega_1 \in (0, 1)$ such that for any $\varepsilon > 0$ and $L \in \mathbb{N}$

$$\mathbb{P}_{\varepsilon, L} \{|\Phi_t^\circ(Q_0^1, P_1^*) - \Phi_t^\circ(Q_0^2, P_1^*)| \leq \rho_0 |Q_0^1 - Q_0^2| \mid (Q_0^1, Q_0^2) = (q^1, q^2)\} \geq \omega_1.$$

By triangle inequality, the pathwise error bound of the leap-frog integrator (5) and compactness of A , there exist $\varepsilon_1 > 0$ and $\rho_1 \in [0, 1)$ such that

$$\mathbb{P}_{\varepsilon, L} \left\{ |\hat{\Phi}_{\varepsilon, L}^\circ(Q_0^1, P_1^*) - \hat{\Phi}_{\varepsilon, L}^\circ(Q_0^2, P_1^*)| \leq \rho_1 |Q_0^1 - Q_0^2| \mid (Q_0^1, Q_0^2) = (q^1, q^2) \right\} \geq \omega_1$$

for $\varepsilon \in (0, \varepsilon_1)$ and $L \in \mathbb{N}$ satisfying $\varepsilon L = t$. Using the Hamiltonian error bound of the leap-frog integrator (6) and compactness of A , it follows from (7) that there exist $\varepsilon_2 \in (0, \varepsilon_1]$ and $\omega_2 \in (0, \omega_1)$ such that

$$\mathbb{P}_{\varepsilon, L} \left\{ Q_1^1 = \hat{\Phi}_{\varepsilon, L}^\circ(Q_0^1, P_1^*), Q_1^2 = \hat{\Phi}_{\varepsilon, L}^\circ(Q_0^2, P_1^*) \mid (Q_0^1, Q_0^2) = (q^1, q^2) \right\} \geq 1 - \omega_2$$

for $\varepsilon \in (0, \varepsilon_2)$ and $L \in \mathbb{N}$ satisfying $\varepsilon L = t$. Noting that the event

$$\begin{aligned} \{|Q_1^1 - Q_1^2| \leq \rho_1 |Q_0^1 - Q_0^2|\} &\supseteq \left\{ |\hat{\Phi}_{\varepsilon, L}^\circ(Q_0^1, P_1^*) - \hat{\Phi}_{\varepsilon, L}^\circ(Q_0^2, P_1^*)| \leq \rho_1 |Q_0^1 - Q_0^2| \right\} \\ &\cap \left\{ Q_1^1 = \hat{\Phi}_{\varepsilon, L}^\circ(Q_0^1, P_1^*), Q_1^2 = \hat{\Phi}_{\varepsilon, L}^\circ(Q_0^2, P_1^*) \right\}, \end{aligned}$$

by Fréchet's inequality

$$\inf_{q^1, q^2 \in S} \mathbb{P}_{\varepsilon, L} \{ |Q_1^1 - Q_1^2| \leq \rho_1 |Q_0^1 - Q_0^2| \mid (Q_0^1, Q_0^2) = (q^1, q^2) \} \geq \omega_1 - \omega_2 > 0. \quad (15)$$

Consider $\delta > 0$, $u_0 > \inf_{q \in S} U(q)$ and $u_1 < \sup_{q \in S} U(q)$ with $u_0 < u_1$, and define the sets $A_\ell = L_\ell(U_S) \times L_{u_1 - \ell}(K) \subset L_{u_1}(E)$ for $\ell \in (u_0, u_1)$. As continuity and convexity of U_S imply that it is a closed function, its level sets $L_\ell(U_S)$ for $\ell \in (u_0, u_1)$ are closed. Moreover, under the assumptions on U and S , it follows that these levels are compact with positive Lebesgue measure. To iterate the argument in (15), note first that if $(q, p) \in A_\ell$, Property 2 and continuity of U and the mapping $t \mapsto \Phi_t^\circ(q, p)$ imply that $\Phi_t^\circ(q, p) \in L_{u_1}(U_S)$ for any $t \in \mathbb{R}_+$. Due to time discretization, we only have from (6) that $\hat{\Phi}_{\varepsilon, L}^\circ(q, p) \in L_{u_1 + \eta_0}(U)$ for some small $\eta_0 > 0$. Set $n_0 = \inf\{n \geq 1 : \rho_1^n \sup_{q, q' \in S} |q - q'| \leq \delta\}$ and take $v_0 \in (u_0, u_1)$, $k_0 > 0$, $\eta_0 > 0$ small enough such that $v_0 + (n_0 + 1)k_0 + n_0\eta_0 < u_1$ holds. Therefore we can conclude that

$$\inf_{q^1, q^2 \in L_{v_0}(U_S)} \mathbb{P}_{\varepsilon, L} \{ |Q_{n_0}^1 - Q_{n_0}^2| \leq \delta \mid (Q_0^1, Q_0^2) = (q^1, q^2) \} \geq (\omega_1 - \omega_2)^{n_0} > 0$$

and (14) follows. \square

C Proofs of Theorems 1 and 2

Proof of Theorem 1. For any $\delta > 0$, we can apply Proposition 1 with $u_0 = \ell_0$ and any $u_1 \in (\ell_0, \sup_{q \in S} U(q))$; the following adopts the notation in the conclusion of Proposition 1. This proof follows the arguments in [Jacob et al., 2017, Proposition 3.4] with modifications to suit our setup. For $\varepsilon \in (0, \min\{\tilde{\varepsilon}, \bar{\varepsilon}\})$ and $L \in \mathbb{N}$ satisfying $\varepsilon L < \bar{\varepsilon} \bar{L}$, it follows from assumption (8) that the coupled transition kernel $\bar{K}_{\varepsilon, L}$ satisfies the geometric drift condition

$$\bar{K}_{\varepsilon, L}(\bar{V})(q, q') \leq \lambda \bar{V}(q, q') + b$$

for all $q, q' \in \mathbb{R}^d$ with $\bar{V}(q, q') = \{V(q) + V(q')\}/2$ as the bivariate Lyapunov function. Iterating gives $\bar{K}_{\varepsilon, L}^{n_0}(\bar{V})(q, q') \leq \lambda^{n_0} \bar{V}(q, q') + b/(1 - \lambda)$. For $(q, q') \notin L_{\ell_0}(U_S) \times L_{\ell_0}(U_S)$ which implies $(q, q') \notin L_{\ell_1}(V) \times L_{\ell_1}(V)$, we have $\bar{V}(q, q') \geq (1 + \ell_1)/2$. Hence

$$\bar{K}_{\varepsilon, L}^{n_0}(\bar{V})(q, q') \leq \lambda_0 \bar{V}(q, q') \quad (16)$$

with $\lambda_0 = \lambda^{n_0} + 2b(1 - \lambda)^{-1}(1 + \ell_1)^{-1} < 1$ for all $(q, q') \notin L_{\ell_0}(U_S) \times L_{\ell_0}(U_S)$. Define the subsampled Markov chains $(\tilde{Q}_n^1)_{n \geq 0}, (\tilde{Q}_n^2)_{n \geq 0}$ as $\tilde{Q}_n^1 = Q_{n_0 n}^1, \tilde{Q}_n^2 = Q_{n_0 n}^2$ and the corresponding relaxed meeting time as $\tilde{\tau}_\delta = \inf\{n \geq 0 : |\tilde{Q}_n^1 - \tilde{Q}_n^2| \leq \delta\}$. For integers $n, j \geq 0$, consider the decomposition

$$\mathbb{P}_{\varepsilon, L}(\tilde{\tau}_\delta > n) = \mathbb{P}_{\varepsilon, L}(\tilde{\tau}_\delta > n, N_{n-1} \geq j) + \mathbb{P}_{\varepsilon, L}(\tilde{\tau}_\delta > n, N_{n-1} < j) \quad (17)$$

where N_n denotes the number of times the coupled chain $(\tilde{Q}_k^1, \tilde{Q}_k^2)_{k \geq 0}$ visits $L_{\ell_0}(U_S) \times L_{\ell_0}(U_S)$ by time n (with $N_{-1} = 0$). For the first term, it follows from (14) that

$$\mathbb{P}_{\varepsilon, L}(\tilde{\tau}_\delta > n, N_{n-1} \geq j) \leq (1 - \omega)^j. \quad (18)$$

To bound the second term, we define

$$B = \max \left\{ 1, \frac{1}{\lambda_0} \sup_{(q, q') \in L_{\ell_0}(U_S) \times L_{\ell_0}(U_S)} \frac{\bar{K}_{\varepsilon, L}^{n_0}(\bar{V})(q, q')}{\bar{V}(q, q')} \right\} \leq \frac{1}{\lambda_0} \left\{ \lambda^{n_0} + \frac{b}{1 - \lambda} \right\} \quad (19)$$

and apply Markov's inequality to obtain

$$\begin{aligned} \mathbb{P}_{\varepsilon, L}(\tilde{\tau}_\delta > n, N_{n-1} < j) &\leq \mathbb{P}_{\varepsilon, L} \left(\mathbb{I}_{D_\delta^c}(\tilde{Q}_n^1, \tilde{Q}_n^2) B^{-N_{n-1}} \geq B^{-(j-1)} \right) \\ &\leq B^{j-1} \mathbb{E}_{\varepsilon, L} \left[\mathbb{I}_{D_\delta^c}(\tilde{Q}_n^1, \tilde{Q}_n^2) B^{-N_{n-1}} \right] \\ &\leq B^{j-1} \mathbb{E}_{\varepsilon, L} \left[B^{-N_{n-1}} \bar{V}(\tilde{Q}_n^1, \tilde{Q}_n^2) \right] \\ &= \lambda_0^n B^{j-1} \mathbb{E}_{\varepsilon, L} [M_n] \end{aligned} \quad (20)$$

where $M_n = \lambda_0^{-n} B^{-N_{n-1}} \bar{V}(\tilde{Q}_n^1, \tilde{Q}_n^2)$. Let \mathcal{F}_n denote the σ -algebra generated by the random variables $(\tilde{Q}_k^1, \tilde{Q}_k^2)_{0 \leq k \leq n}$. We now establish that $(M_n, \mathcal{F}_n)_{n \geq 0}$ is a sub-martingale. Suppose $(\tilde{Q}_n^1, \tilde{Q}_n^2) \notin L_{\ell_0}(U_S) \times L_{\ell_0}(U_S)$, in which case $N_n = N_{n-1}$, and applying (16) gives

$$\mathbb{E}_{\varepsilon, L} [M_{n+1} \mid \mathcal{F}_n] = \lambda_0^{-n-1} B^{-N_{n-1}} \mathbb{E}_{\varepsilon, L} [\bar{V}(\tilde{Q}_{n+1}^1, \tilde{Q}_{n+1}^2) \mid \tilde{Q}_n^1, \tilde{Q}_n^2] \leq M_n.$$

For other case $(\tilde{Q}_n^1, \tilde{Q}_n^2) \in L_{\ell_0}(U_S) \times L_{\ell_0}(U_S)$, we have $N_n = N_{n-1} + 1$ hence it follows from (19) that

$$\mathbb{E}_{\varepsilon, L} [M_{n+1} \mid \mathcal{F}_n] = \lambda_0^{-n} B^{-N_{n-1}-1} \bar{V}(\tilde{Q}_n^1, \tilde{Q}_n^2) \frac{\mathbb{E}_{\varepsilon, L} [\bar{V}(\tilde{Q}_{n+1}^1, \tilde{Q}_{n+1}^2) \mid \tilde{Q}_n^1, \tilde{Q}_n^2]}{\lambda_0 \bar{V}(\tilde{Q}_n^1, \tilde{Q}_n^2)} \leq M_n.$$

By the sub-martingale property and assumption (8), $\mathbb{E}_{\varepsilon, L}[M_n] \leq E_{\varepsilon, L}[M_0] \leq \{(\lambda+1)\pi_0(V) + b\}/2$. Therefore combining (17), (18), (20) and noting that the relaxed meeting times satisfy $\{\tau_\delta > n_0 n\} \subseteq \{\tilde{\tau}_\delta > n\}$ give

$$\mathbb{P}_{\varepsilon, L}(\tau_\delta > n_0 n) \leq \mathbb{P}_{\varepsilon, L}(\tilde{\tau}_\delta > n) \leq (1 - \omega)^j + \frac{1}{2}\{(\lambda + 1)\pi_0(V) + b\}\lambda_0^n B^{j-1}.$$

Since $\lambda_0 < 1$, there exists $m_0 \in \mathbb{N}$ such that $\lambda_0 B^{1/m_0} < 1$. For integer $n \geq m_0$, we can choose $j = \lceil n/m_0 \rceil$ to obtain

$$\mathbb{P}_{\varepsilon, L}(\tau_\delta > n_0 n) \leq \{(1 - \omega)^{1/m_0}\}^n + \frac{1}{2}\{(\lambda + 1)\pi_0(V) + b\}(\lambda_0 B^{1/m_0})^n$$

which implies (9). \square

Proof of Theorem 2. For any $\delta > 0$, we can apply Proposition 1 with $u_0 = \ell_0$ and any $u_1 \in (\ell_0, \sup_{q \in S} U(q))$; the following adopts the notation in the conclusion of Proposition 1. Suppose that the coupled chain $(X_n, Y_n)_{n \geq 0}$ is initialized at $(X_0, Y_0) = (x, y) \in S_0 \times S_0$ and evolves according to $(X_n, Y_n) \sim \bar{K}_{\varepsilon, L, \sigma}((X_{n-1}, Y_{n-1}), \cdot)$ for all integer $n \geq 1$, $\sigma > 0$ and some $\varepsilon \in (0, \bar{\varepsilon})$, $L \in \mathbb{N}$ satisfying $\varepsilon L < \bar{\varepsilon} \bar{L}$ (note that this differs from the time shift presented in Algorithm 2). Let $\{I_n = 1\}$ denote the event that the coupled Hamiltonian Monte Carlo kernel is sampled from the mixture (11) at time n , i.e. $(I_n)_{n \geq 1}$ is a sequence of independent Bernoulli random variables with probability of success $1 - \gamma \in (0, 1)$. By conditioning on the event $\cap_{n=1}^{n_0} \{I_n = 1\}$, it follows from the proof of Proposition 1 that there exist $n_0 \in \mathbb{N}$ and $\omega \in (0, 1)$ such that

$$\inf_{x, y \in S_0} \mathbb{P}_{\varepsilon, L, \sigma} \{(X_{n_0}, Y_{n_0}) \in D_\delta \cap S \times S \mid (X_0, Y_0) = (x, y)\} \geq (1 - \gamma)^{n_0} \omega. \quad (21)$$

Now conditioning on the events $\{(X_{n_0}, Y_{n_0}) \in D_\delta \cap S \times S\}$ and $\{I_{n_0+1} = 0\}$, for any $\sigma > 0$ and $\theta_1 \in (0, 1)$, the approximation (10) allows us to select $\delta > 0$ small enough so that the maximal coupling within the coupled random walk Metropolis–Hastings kernel \bar{K}_σ proposes the same value $X_{n_0+1}^* = Y_{n_0+1}^*$ with probability at least $1 - \theta_1$. For any $\theta_2 \in (0, 1)$, we now establish that the probability of accepting the proposed value satisfies

$$\mathbb{P}_{\varepsilon, L, \sigma} \{X_{n_0+1} = X_{n_0+1}^* \mid I_{n_0+1} = 0, (X_{n_0}, Y_{n_0}) \in D_\delta \cap S \times S, (X_0, Y_0) = (x, y)\} \geq 1 - \theta_2 \quad (22)$$

if $\sigma > 0$ is sufficiently small. We can rewrite the above probability as

$$\mathbb{P}_{\varepsilon, L, \sigma} \left\{ U_{n_0+1} \leq \min \left[1, \frac{\pi(X_{n_0} + \sigma Z_{n_0+1})}{\pi(X_{n_0})} \right] \mid (X_{n_0}, Y_{n_0}) \in D_\delta \cap S \times S, (X_0, Y_0) = (x, y) \right\}$$

where $U_{n_0+1} \sim \mathcal{U}[0, 1]$ and $Z_{n_0+1} = X_{n_0+1}^*/\sigma \sim \mathcal{N}(0, I_d)$ are independent. By Assumption 4, we have

$$\min \left[1, \frac{\pi(v + \sigma z)}{\pi(v)} \right] \geq \min \left[1, \exp \left\{ -\frac{1}{2} \sigma^2 \beta |z|^2 - \sigma \nabla U(v)^\top z \right\} \right]$$

for all $v, z \in \mathbb{R}^d$. Define $\varphi_1(\sigma, v, z) = \exp\{-\sigma^2 \beta |z|^2/2\}$, $\varphi_2(\sigma, v, z) = \exp\{-\sigma \nabla U(v)^\top z\}$ and $B_0(r) = \{z \in \mathbb{R}^d : |z| \leq r\}$ for some $r > 0$. Note that for each $(v, z) \in S \times B_0(r)$ and $i = 1, 2$, $\sigma \mapsto \varphi_i(\sigma, v, z)$ is a monotone function and $\lim_{\sigma \rightarrow 0} \varphi_i(\sigma, v, z) = 1$. Since $S \times B_0(r)$ is compact and ∇U is continuous, it follows from Dini's theorem that $\lim_{\sigma \rightarrow 0} \inf_{v \in S, z \in B_0(r)} \varphi_i(\sigma, v, z) = 1$. By conditioning on the events $\{X_{n_0} \in S\}$ and $\{Z_{n_0+1} \in B_0(r)\}$, we have

$$\left\{ U_{n_0+1} \leq \min \left[1, \frac{\pi(X_{n_0} + \sigma Z_{n_0+1})}{\pi(X_{n_0})} \right] \right\} \supseteq \left\{ U_{n_0+1} \leq \min \left[1, \prod_{i=1}^2 \inf_{v \in S, z \in B_0(r)} \varphi_i(\sigma, v, z) \right] \right\}.$$

The claim in (22) follows by taking $r > 0$ sufficiently large and $\sigma > 0$ sufficiently small. Therefore by symmetry of the coupled chains and Fréchet's inequality, for any $\theta \in (0, 1)$, there exists $\bar{\sigma} > 0$ such that for any $\sigma \in (0, \bar{\sigma})$

$$\mathbb{P}_{\varepsilon, L, \sigma} \{X_{n_0+1} = Y_{n_0+1} \mid I_{n_0+1} = 0, (X_{n_0}, Y_{n_0}) \in D_\delta \cap S \times S, (X_0, Y_0) = (x, y)\} \geq 1 - \theta. \quad (23)$$

Combining (21) with (23) gives

$$\inf_{x,y \in S_0} \bar{K}_{\varepsilon,L,\sigma}^{n_0+1}((x,y), D) \geq (1-\gamma)^{n_0} \omega \gamma (1-\theta) > 0 \quad (24)$$

for $\varepsilon \in (0, \bar{\varepsilon})$, $L \in \mathbb{N}$ satisfying $\varepsilon L < \bar{\varepsilon} \bar{L}$ and $\sigma \in (0, \bar{\sigma})$, where $D = \{(x, y) \in \mathbb{R}^d \times \mathbb{R}^d : x = y\}$. With (24), the claim in (13) follows using the same arguments in the proof of Theorem 1 since the marginal mixture kernel $K_{\varepsilon,L,\sigma}$ satisfies the geometric drift condition

$$\begin{aligned} K_{\varepsilon,L,\sigma}(V)(x) &= (1-\gamma)K_{\varepsilon,L}(V)(x) + \gamma K_\sigma(V)(x) \\ &\leq (1-\gamma)\{\lambda V(x) + b\} + \gamma\{Q_\sigma(V)(x) + V(x)\} \\ &\leq \lambda_0 V(x) + b_0 \end{aligned}$$

for all $x \in \mathbb{R}^d$ and $\sigma \in (0, \min\{\tilde{\sigma}, \bar{\sigma}\})$, where $\lambda_0 = (1-\gamma)\lambda + \gamma(1+\mu) \in (0, 1)$ and $b_0 = (1-\gamma)b + \gamma\mu < \infty$.

□